Conversion of Digital Numbers of the HSS Sensor TIR Images into Radiance: Uncertainty Evaluation

Leidiane L. Andrade[1], Ruy M. Castro[1] Lênio S. Galvão [2]

[1] Instituto de Estudos Avançados - IEAv/DCTA, Caixa Postal 6044 – 12.231-970 – São José dos Campos - SP, Brasil
Leidiane.andrade@ieav.cta.br, rmcastro@ieav.cta.br
[2] Instituto Nacional de Pesquisas Espaciais – INPE, Caixa Postal 515 - 12227-010 - São José dos Campos - SP, Brasil
lenio@dsr.inpe.br

Abstract

One goal of remote sensing in the thermal infrared region is the determination of the temperature and surface emissivity in urban areas. For the conversion of Digital Numbers (DN) into radiance values, it is important to characterize the uncertainty sources associated with the process of data acquisition itself and with other important factors such as the atmospheric correction. This study addresses this topic. Results showed that the uncertainties due to the atmospheric influence was the factor that most contributed to the final data uncertainty (3%), followed by the uncertainties associated with the radiance determination (0.5%). As a result, the final uncertainties in temperature data obtained for each pixel was 1.8 ° C, which varied with the studied urban material.

Keywords: Thermal Remote Sensing, Emissivity, Temperature.

1. Introduction

The thermal remote sensing has been used in several urban studies due to the possibility of obtaining temperature and emissivity data on a per-pixel basis and of associating them with the use of the urban space. However, to use these data, it is essential to understand the process of thermal imaging and the steps applied to obtain the image in physical quantities such as radiance, temperature or emissivity.

The HSS (Hyperspectral Scanner System) sensor operates in 50 bands (or channels) in the visible, near-infrared, shortwave infrared and thermal spectral intervals. The six thermal infrared bands are positioned between 8 and 12.5 μm (Moreira *et al*., 2005; Sensytech, 2004). In addition, the HSS sensor has two reference blackbodies (RBB1 and RBB2), which are used as references of thermodynamic temperature (minimum and maximum) for calibration purposes. The image of each band of the HSS sensor is quantified in Digital Number (DN) of the voltage/current provided by the detector element and associated electronics, which is related to the signal generated by emitted and/or reflected radiation (from the surface and atmosphere), combined with the gain and offset factors adjusted by the operator.

Therefore, the aim of this paper is to evaluate the uncertainties in the process of estimating surface temperature. This includes the methodology to convert DN's of

the HSS sensor Thermal Infrared (TIR) images into radiance values. Furthermore, the resultant radiance images were corrected for the atmospheric effects before estimating the surface temperature and relative spectral emissivity. Finally, using this approach, an instrumental uncertainty was obtained.

2. Methodology

The methodology involved several sequential steps. The first step was to assess the quality of the images, including the possible presence of strong variations in brightness associated with the geometry of data acquisition. In the second step, we evaluated the adjustments of the thermodynamic temperatures of the reference blackbodies and its correlation with DN's, to check for possible occurrence of pixels with abnormal values. In the third step, we observed the fluctuations of the DN's reference blackbodies to estimate the noise in the image, based on the work of Castro *et al*. (2005; 2007). Thus, the noise was determined by the ratio of standard deviation of DN's reference blackbody (RBB2), adjusted to the highest temperature, and the mean value of its DN's.

Finally, to convert the DN's into radiance values, it was necessary to conduct a thermal characterization of the image generated. This process started with the determination of the spectral exitance of the blackbody through the Planck's equation (Schott, 1997). After that, to estimate the spectral exitance of the RBB's, we used the reference blackbody thermodynamic temperatures, T_{RBB}, thus:

$$L_{RBB,b}(T_{RBB},\lambda)=\int_{\lambda_1}^{\lambda_2}\frac{1}{\pi}\cdot\frac{2\pi\cdot h\cdot c^2}{\lambda^5\left[e^{h\cdot c/\lambda\cdot k\cdot T_{RBB}}-1\right]}\cdot SRF_b(\lambda)\cdot\varepsilon_{RBB}(\lambda)\,\mathrm{d}\lambda \quad (1)$$

To calculate the spectral radiance of the RBB´s, L_{RBB}, by the means of their exitance in a given thermodynamic temperature, T_{RBB}, we assumed that: a) the surface of the RBB´s has an isotropic emission, b) the emissivities of the RBB´s, $\varepsilon_{RBB}(\lambda)$, are equal to 1; c) and the transmittance of the optical path in the sensor is maximum, i.e., equal to 1, and further taken into account by the Spectral Response Function, *SRF*, of each band, *b*.

The parameters, $Gain_b$ and $Offset_b$, for each band, were obtained through an adjustment of a linear fit of the estimated radiance as a function of DN's for both RBB´s. The value obtained was the at-sensor radiance.

Then, to obtain surface radiance images, L_s, it was necessary to evaluate and correct the effects of the atmosphere (downwelling radiance, L_d; material emissivity, ε_{mat}; transmittance, τ; and path radiance, L_{pth}) for each band, as described by the equation.

$$L_{s,b}=\tau_b\cdot L_{e,b}+\tau_b\cdot\left[L_{d,b}\cdot\left(1-\varepsilon_{mat,b}\right)\right]+L_{pth,b} \quad (2)$$

Thereby, by using the methodology explained by Andrade *et al*. (2012), the downwelling radiance, transmittance, and path radiance was estimated. These parameters considered the Spectral Response Function, *SRF*, of each band, *b*, of the sensor. For example, to obtain a transmittance factor, τ_b, we used the equation:

$$\tau_b=\frac{\int_{\lambda_1}^{\lambda_2}SRF_b(\lambda)\cdot\tau(\lambda)\cdot\mathrm{d}\lambda}{\int_{\lambda_1}^{\lambda_2}SRF_b(\lambda)\cdot\mathrm{d}\lambda} \quad (3)$$

The same was performed to $L_{a,b}$ and $L_{d,b}$, which were used in the radiative transfer model described by Equation (2).

For sensors with n thermal bands there are n equations with n+ 1 unknown. By measuring the radiance in n bands, we cannot obtain n spectral emissivity plus surface temperature values (Gillespie et al., 1998). In this case, field measurement should be carried out. However, if one does not have these data, an alternative is to use some method for establishing certain links between the emissivity and temperature. Therefore, to estimate the emissivity and temperature images, we used the Emissivity Normalization (NOR) technique. This method assumes a constant emissivity in all bands for a given pixel. The temperature, for each band, is then estimated. After that, the maximum temperature of all thermal bands is considered as the surface temperature. Using Equation (2), the emissivity for all bands was derived. The constant emissivity selected was 0.98, which is closer to that of water and vegetation.

Uncertainty Evaluation

Sources of uncertainties of the methodology for determining the surface temperature and emissivity were evaluated from: thermodynamic temperature of RBB´s; blackbodies digital numbers (DN); emissivity of the blackbody; Spectral Response Function ; conversion of DN into radiance; atmospheric influence; application of NOR method; and heterogeneity of the material surface.

The evaluation of the stability of the temperature of the blackbodies was performed by monitoring the measurements, in each row, across the image. Thus, the standard deviation was defined as the uncertainty of the measurement. The same procedure was applied to the DN of each RBB.

To estimate the uncertainty associated with the conversion of DN into radiance, we evaluated the propagation of the uncertainties of the adjusted parameters in the linear regression. This uncertainty also includes the uncertainty related to the emissivity of the blackbodies and that due to the Spectral Response Function that was estimated to from the information provided by the HSS´ manufacturer(0.5%; ie, 0.005).

Then we evaluated the influence of the atmosphere (Equation 2) using as support data obtained from meteorological station and radiosonde; the altitude recorded by the GPS system sensor; the sensor view zenith angle; and the approximations resultant from the atmospheric model select to correct the images.

The NOR method implemented in the ENVI software was used to convert the radiance into temperature and emissivity. As this method is "iterative", the propagation of uncertainties is complicated. Therefore, the uncertainty was estimated by applying the method by: (a) first using the value of the radiance obtained plus its uncertainty; and (b) second, subtracting the radiance from the uncertainty. Then the uncertainty for each pixel was estimated by half of the difference of these two cases.

3. Results

We used nadir images acquired over the urban area of São José dos Campos (Brazilian state of São Paulo), in nighttime period of May 30th 2006. The Instantaneous Field of View (IFOV) was adjusted to 2.5 mrad and the scanning frequency to 25 Hz. Then, the maximum and minimum temperatures of the reference blackbody (RBB) were set up to 45 and 17 °C, respectively. The spatial resolution was

2.9 m at nadir. The swath width was 2.1 km because of the 86° Field of View (FOV) and the flight altitude of 1736 m.

The images used in this work had a good visual quality. When evaluating the stability of the thermodynamic temperature of the reference blackbodies throughout the imaging, it was found that they were stable with a variation of 0.2 °C around the mean (Figure 1). The estimated uncertainty was 0.02 °C due to digitalization of the data. The DN values of the reference blackbody measured by the detectors varied in the 100-200 range. This variation was probably due to the inherent noise of the sensor system. The uncertainty ranged from 0.4 to 0.9 DN in the 6 bands.

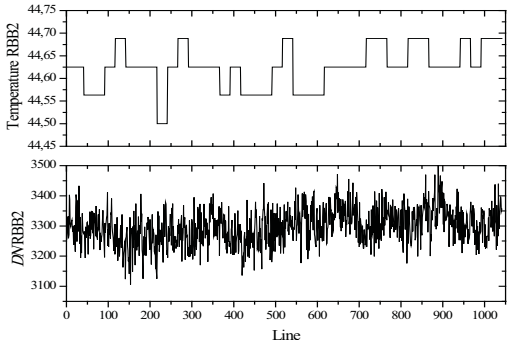

Figure 1: a) Evaluation the stability of the thermodynamic temperature measured by thermocouple of the RBB2; b) DN of the RBB2 for band 50.

Thus, the temperature data from the reference blackbodies was used to estimate the radiance (Equation 1). The relative uncertainties of 0.5% were due to the estimated uncertainty of the emissivity of the RBB and SRF. The parameters *Gain* and *Offset* of thermodynamic temperature of reference blackbodies are listed in Table 1.

Table 1: Parameters for the bands of the spectrum emitted.

Band	Central Wavelength µm	*Offset* W / m^2·sr·nm	*Gain*·10^{-3} W / m^2·sr·nm
45	8.18	4.57 ± 0.07	2.361 ± 0.033
46	8.68	6.51 ± 0.05	1.710 ± 0.025
47	9.16	6.37 ± 0.06	1.830 ± 0.028
48	9.80	7.06 ± 0.06	1.542 ± 0.025
49	10.81	7.14 ± 0.06	1.702 ± 0.031
50	12.02	7.24 ± 0.05	1.190 ± 0.024

Thus, the value of the radiance of each pixel of the image had a relative uncertainty of 0.5%. To estimate the atmospheric influence, we first determine the downwelling radiance, L_d (λ). For this purpose, it was necessary to estimate the emissivity and temperature of the sky using the data dew point temperature (15.4 ± 0.5) °C and the dry bulb temperature (18.1 ± 1.0) °C, obtained from the meteorological station located at the Airport of Sao Jose dos Campos - Professor Urbano Ernesto Stumpf. The estimated temperature and emissivity values of the sky were (0.84 ± 0.02) and (5.4 ± 2.0) °C, respectively, after applying the Berdahl and Fromberg method (Pérez-Garcia, 2004). The relative uncertainty of the downwelling radiance was 2.7%. However, in relation to other parameters, its importance was very small because the reflectance, in the thermal wavelength, of the land surface was estimated in 2% (Table 2).

Then, the spectral transmittance, $\tau(\lambda)$, and spectral path radiance, $L_{pth}(\lambda)$, were calculated using the PcModWin/MODTRAN. The atmospheric model used was Tropical. The season was assumed as autumn/winter due to the period of year. The concentration of carbon dioxide (CO_2) was 360 ppm (CONWAY et al., 1994). The adopted model was urban/aerosol with visibility of 40 km. We used 33 atmospheric layers, the maximum number allowed by the program, with layers closer to the surface, due to the flight altitude of 1736 m. A refinement of the data was performed using relative humidity of the atmospheric profile from radiosonde data obtained by the Instituto Astronômico e Geofísico da Universidade de São Paulo (IAG/USP) in the Campo de Marte Airport, nearest to the area covered by the imaging. These parameters were weighted for the Spectral Response Function, *SRF*, of each band (Table 2). Through various tests on the parameters involved in atmospheric modeling, we calculated the relative uncertainty for the transmittance and path radiance as 3%.

Table 2: Atmospheric parameters used in thermal image correction.

Band	Central Wavelength (μm)	Downwelling Radiance ($W/m^2 \cdot \mu m \cdot sr$)	Path Radiance ($W/m^2 \cdot \mu m \cdot sr$)	Transmittance
45	8.18	1.574	3.630	0.536
46	8.68	1.682	2.445	0.707
47	9.16	1.756	2.138	0.752
48	9.80	1.812	2.050	0.767
49	10.81	1.821	2.326	0.730
50	12.02	1.736	3.137	0.607

In the atmospheric correction, the radiance values of pixels in a given band decreases by a constant value. However, the radiance of the pixels of the image remains correlated. After that, the images were converted into emissivity and temperature by the NOR method, for the analysis of the main urban materials of the study area. Results showed that the spectral emissivity was consistent with the literature. Among the artificial materials, the concrete had the highest temperature, followed by the asphalt, while the temperature of the galvanized steel was the lowest one. The average temperature of the vegetation was 15 °C with standard deviation of 2.5 °C (Table 3). The temperature estimated by the NOR method showed that the spectral emissivity was consistent with the literature for the studied materials.

Table 3: Uncertainties of the temperature estimated by the NOR method.

Materials	Temperature (°C)	
	Mean	σ
Asphalt	21.00	1.81
Concrete pavement	23.40	1.34
Red Tile roof	13.77	1.23
Fiber cement roof	15.52	1.04
Galvanized Steel Gray	12.41	1.37
Grass	15.10	2.49

In general, it was found that the uncertainty in the temperature data at each pixel was approximately 1.8 °C, varying according to the analyzed material. By comparing the standard deviation of the temperature, for some materials, with the estimated uncertainty for temperature, it was found that both parameters had the same magnitude. The uncertainty analysis of the data emissivity is much more

complex, because the NOR method results in relative emissivity data (spectrum shape) rather than in absolute emissivity values in each band. Therefore, the estimate of its uncertainty requires further studies.

3. Conclusion

The NOR method showed consistent results in estimating the relative spectral emissivity of materials of interest, specifically in urban areas. Thus, it was evident the great potential of the HSS images in the emitted spectrum, which combines the high spatial resolution and a better spectral resolution than most of the orbital satellite sensors to study the emissivity of urban materials.

In relation to the final uncertainty of the estimated temperature, results showed that the atmosphere influence was the factor that most contributed to the final uncertainty of the data, followed by the uncertainties in the radiance determination for each pixel. Thus, the final uncertainties in temperature data obtained for each pixel of the image was 1.8 °C, varying according to the analyzed urban material.

References

Andrade, L. L.; Castro, R. M. Galvão, L. S. (2012), "Conversão dos números digitais de imagens TIR do sensor HSS para radiância e estimativa da temperatura e emissividade." *Revista Brasileira de Cartografia.* In pres.

Castro, R.M.; Moreira, R.C.; Esposito, E.S.C.; Lucca, E.V.D. (2005), "Avaliação do ruído em sensores eletroópticos: abordagem da imagem escura no HSS". In: São José dos Campos: INPE. *Proceedings of XII Simpósio Brasileiro de Sensoriamento Remoto*, Goiânia, Brasil, pp. 355-362.

Castro, R.M.; Moreira, R.C.; Esposito, E.S.C.; (2007), "Avaliação em laboratório do sensor HSS". In: São José dos Campos: INPE. *Proceedings of XIII Simpósio Brasileiro de Sensoriamento Remoto*, Florianópolis, Brasil, pp. 6443-6448.

Conway, T. J.; Tans, P. P.; Waterman, L. S.; Thoning, K. W.; Kitzis, D.; Masarie, K. A.; Zhang, N. (1994), "Evidence for inter-annual variability of the carbon cycle from the National Oceanic and Atmospheric Administration/Climate Monitoring and Diagnostics Laboratory Global Air Sampling Network". *Journal of Geophysical Research-Atmospheres*, Vol. 99(D11): 22831-22855.

Gillespie, A.; Rokugawa, S.; Matsunaga, T.; Cothern, J. S.; Hook, S. J.; Kahle, A. B. (1998), "A temperature and emissivity separation algorithm for Advanced Spaceborne Thermal Emission and Reflection Radiometer (ASTER) images". *IEEE Transactions on Geosciences and Remote Sensing*, Vol. 36(4), pp. 1113-1126.

Moreira, R.C.; Castro, R.M.; Esposito, E.S.C.; Lucca, E.V.D. (2005) "Sensor hiperespectral HSS: sumário das características técnicas". n: São José dos Campos: INPE. *Proceedings of XII Simpósio Brasileiro de Sensoriamento Remoto*, Goiânia, Brasil, pp. 4517-4524.

Pérez-Garcia, M. Simplified modeling of the nocturnal clear sky atmospheric radiation for environmental applications. Ecological Modeling, v.180, n.2-3, p.395-406, 2004.

Schott, J.R. (1997), Remote sensing: the image chain approach. New York: Oxford University Press. 401p.

Sensytech, Inc. AA5201 Airborne Hyperspectral Scanner System: operator manual. Ann Arbor, v. 1, 2004. 104p. (Sensytech MN52011A Rev.2).